Behavioral/Cognitive

Minimal Phrase Composition Revealed by Intracranial Recordings

Elliot Murphy,[1,2] **Oscar Woolnough,**[1,2] **Patrick S. Rollo,**[1,2] **Zachary J. Roccaforte,**[1] **Katrien Segaert,**[3,4] **Peter Hagoort,**[4,5] **and Nitin Tandon**[1,2,6]

[1]Vivian L. Smith Department of Neurosurgery, McGovern Medical School, University of Texas Health Science Center at Houston, Houston, Texas 77030, [2]Texas Institute for Restorative Neurotechnologies, University of Texas Health Science Center at Houston, Houston, Texas 77030, [3]School of Psychology and Centre for Human Brain Health, University of Birmingham, Birmingham B15 2TT, United Kingdom, [4]Max Planck Institute for Psycholinguistics, Nijmegen, 6525 XD Nijmegen, The Netherlands, [5]Donders Institute for Brain, Cognition and Behaviour, Nijmegen, 6525 HR Nijmegen, The Netherlands, and [6]Memorial Hermann Hospital, Texas Medical Center, Houston, Texas 77030

The ability to comprehend phrases is an essential integrative property of the brain. Here, we evaluate the neural processes that enable the transition from single-word processing to a minimal compositional scheme. Previous research has reported conflicting timing effects of composition, and disagreement persists with respect to inferior frontal and posterior temporal contributions. To address these issues, 19 patients (10 male, 9 female) implanted with penetrating depth or surface subdural intracranial electrodes, heard auditory recordings of adjective-noun, pseudoword-noun, and adjective-pseudoword phrases and judged whether the phrase matched a picture. Stimulus-dependent alterations in broadband gamma activity, low-frequency power, and phase-locking values across the language-dominant left hemisphere were derived. This revealed a mosaic located on the lower bank of the posterior superior temporal sulcus (pSTS), in which closely neighboring cortical sites displayed exclusive sensitivity to either lexicality or phrase structure, but not both. Distinct timings were found for effects of phrase composition (210–300 ms) and pseudoword processing (~300–700 ms), and these were localized to neighboring electrodes in pSTS. The pars triangularis and temporal pole encoded anticipation of composition in broadband low frequencies, and both regions exhibited greater functional connectivity with pSTS during phrase composition. Our results suggest that the pSTS is a highly specialized region composed of sparsely interwoven heterogeneous constituents that encodes both lower and higher level linguistic features. This hub in pSTS for minimal phrase processing may form the neural basis for the human-specific computational capacity for forming hierarchically organized linguistic structures.

Key words: **auditory; human; language; phrase structure; semantics**

Significance Statement

Linguists have claimed that the integration of multiple words into a phrase demands a computational procedure distinct from single-word processing. Here, we provide intracranial recordings from a large patient cohort, with high spatiotemporal resolution, to track the cortical dynamics of phrase composition. Epileptic patients volunteered to participate in a task in which they listened to phrases (red boat), word-pseudoword or pseudoword-word pairs (e.g., red fulg). At the onset of the second word in phrases, greater broadband high gamma activity was found in posterior superior temporal sulcus in electrodes that exclusively indexed phrasal meaning and not lexical meaning. These results provide direct, high-resolution signatures of minimal phrase composition in humans, a potentially species-specific computational capacity.

Introduction

How the brain integrates individual word meanings to comprehend multiword utterances is an issue that has vexed the cognitive neuroscience of language for decades (Hagoort, 2020). This linguistic compositional process—the combination of words into larger structures with new and complex meaning—has been referred to as Merge (Chomsky et al., 2019) or Unification (Hagoort, 2013). A simple paradigm for studying complex meaning is the use of minimal phrases, such as in the red-boat paradigm, which focuses on simple combinations of two words and

Received Aug. 2, 2021; revised Jan. 11, 2022; accepted Jan. 18, 2022.

Author contributions: K.S., P.H., and N.T. designed research; E.M., O.W., P.S.R., and Z.J.R. performed research; E.M. and N.T. analyzed data; E.M. wrote the paper.

This work was supported by the National Institute of Neurological Disorders and Stroke Grant NS098981. We thank all the patients who participated in this study; the neurologists at the Texas Comprehensive Epilepsy Program who participated in the care of these patients, and the nurses and technicians in the Epilepsy Monitoring Unit at Memorial Hermann Hospital who helped make this research possible.

The authors declare no competing financial interests.

Correspondence should be addressed to Nitin Tandon at nitin.tandon@uth.tmc.edu.

https://doi.org/10.1523/JNEUROSCI.1575-21.2022

avoids confounds associated with more complex linguistic stimuli (Bemis and Pylkkänen, 2011, 2013; Brennan and Pylkkänen, 2012; Bozic et al., 2015; Flick et al., 2018; Flick and Pylkkänen, 2020; Pylkkänen, 2020). A red boat is interpreted as a boat that is red and not a red object that hosts boat-related properties, with phrases delivering novel syntactic and conceptual formats (Murphy, 2015, 2019; Leivada and Murphy, 2021). Red-boat experiments isolate semantic composition, which in turn encompasses syntactic composition.

Functional neuroimaging studies using the red-boat paradigm implicate the left anterior temporal lobe (ATL), specifically the temporal pole (Antonucci et al., 2008; Lambon Ralph et al., 2012; Wilson et al., 2014; Zhang and Pylkkänen, 2018), inferior frontal regions (Graessner et al., 2021a,b), and posterior temporal regions (Flick and Pylkkänen, 2020; Matchin and Hickok, 2020) as crucial nodes for phrase composition with variations in the timing (180–350 ms postcomposition) and duration (50–100 ms) of their engagement (Kochari et al., 2021). Posterior temporal cortex is more broadly implicated in syntactic comprehension and production (Duffau et al., 2014; Artoni et al., 2020; Matchin and Hickok, 2020; Lopopolo et al., 2021; Graessner et al., 2021b). The left posterior temporal lobe and angular gyrus show greater activity for sentences than word lists and for phrases than words, making them candidate regions for the retrieval of phrasal templates (Hagoort, 2003, 2017; Brennan et al., 2016; Matchin and Hickok, 2020). According to a range of parsing models, adjective-noun syntax is also constructed predictively (Berwick et al., 2019), and anticipatory amplitude increases have been isolated jointly to the alpha/beta bands (Gastaldon et al., 2020).

Phrase composition is a rapid process that is likely dependent on finely organized sets of distributed cortical substrates. Previous work using the red-boat paradigm has been limited by spatiotemporal resolution. Using recordings from intracranial electroencephalography (iEEG), with depth electrodes penetrating gray matter or electrodes located on the cortical surface, we conducted a study of minimal phrase composition with auditory presentations of the red-boat paradigm, building directly and using stimuli from an established design (Bemis and Pylkkänen, 2013). Given our large cohort, we were able to perform a data-driven analysis of iEEG data from the whole brain acquired at unprecedented spatiotemporal resolution.

Most evidence that left ATL and posterior temporal regions are involved in basic composition is from magnetoencephalography (MEG), whereas the evidence supporting a role for inferior frontal gyrus (IFG) mostly comes from functional magnetic resonance imaging (fMRI). Signal loss in fMRI may partly explain the lack of ATL effects in this portion of the imaging literature (because of proximity to sinuses; Olman et al., 2009; Bonner and Price, 2013), yet even within the MEG literature there is variation in the timing of composition effects. This suggests that intracranial recordings can contribute to resolving the spatiotemporal dynamics of phrase processing. Our central research questions concerned the following: (1) the precise localization of composition effects, addressing a current tension in the literature with respect to frontal, temporal, and parietal contributions to minimal phrase processing (Schell et al., 2017; Flick and Pylkkänen, 2020; Graessner et al., 2021a) and (2) the precise timing and duration of composition effects, addressing the above noted variations documented in the literature.

Materials and Methods

Participants. Nineteen patients (10 male, 18–41 years; intelligence quotient, 97 ± 12, two left-handed) participated in the experiment after written informed consent was obtained. All were native English speakers. All experimental procedures were reviewed and approved by the Committee for the Protection of Human Subjects of the University of Texas Health Science Center at Houston, Protocol Number HSC-MS-06–0385.

Electrode implantation and data recording. Data were acquired from either subdural grid electrodes (SDEs; six patients) or stereotactically placed depth electrodes (sEEGs; 13 patients; Fig. 1*B*). SDEs were subdural platinum-iridium electrodes embedded in a silicone elastomer sheet (top hat design, 3 mm diameter cortical contact, PMT), and were surgically implanted via a craniotomy (Conner et al., 2011; Pieters et al., 2013; Tong et al., 2020; Kohlhase et al., 2021). sEEGs were implanted using a Robotic Surgical Assistant (Medtech; Rollo et al., 2020; McCarty et al., 2021). Each sEEG probe (PMT) was 0.8 mm in diameter and had 8–16 electrode contacts. Each contact was a platinum-iridium cylinder, 2.0 mm in length, and separated from the adjacent contact by 1.5–2.43 mm. SDE patients had a number of cortical arrays implanted (mean ± SD, 9 ± 1) with a mean of 146.5 electrodes (SD ± 53.5). sEEG patients had penetrating depth probes (mean 15.1 ± 2.3) with a mean of 199.9 electrodes (SD ± 30.1). Typical coverage was frontotemporal, dictated by location of the epilepsy in the anteromesial temporal lobe in the majority, with parietal and occipital coverage in a number of patients. Following surgical implantation, electrodes were localized by coregistration of preoperative anatomic 3T MRI and postoperative CT scans in Analysis of Functional NeuroImages (Cox, 1996). Electrode positions were projected onto a cortical surface model generated in FreeSurfer (Dale et al., 1999) and displayed on the cortical surface model for visualization (Pieters et al., 2013). Intracranial data were collected during research experiments starting on the first day after electrode implantation for sEEGs and 2 d after implantation for SDEs. Data were digitized at 2 kHz using the NeuroPort recording system (Blackrock Microsystems), imported into MATLAB, initially referenced to the white matter channel used as a reference for the clinical acquisition system and visually inspected for line noise, artifacts, and epileptic activity. iEEG provides uniquely high spatiotemporal resolution recordings and is less susceptible to artifacts (e.g., muscle movements; Flinker et al., 2011; Arya, 2019). Electrodes with excessive line noise or localized to sites of seizure onset were excluded. Each electrode was rereferenced to the common average of the remaining channels. Trials contaminated by interictal epileptic spikes, saccade artefacts, and trials in which participants responded incorrectly were discarded. Electrodes contributing to regions of interest (ROIs) were taken from both SDE and sEEG patients; for instance, we follow previous intracranial work that has included subdural contacts in monitoring activity from posterior temporal sulcus (Uno et al., 2015), although we note that SDE arrays over sulci can also detect activity from adjacent lateral cortex.

Experimental design and statistical analysis. Grammatical noun phrases (red boat) and pseudoword phrases with variable positions of the pseudoword (bleeg boat, red fulg) were used to isolate semantic compositional processing. An adjective-pseudoword condition (red fulg) allowed for the isolation of semantic compositionality and reduced predictability. The inclusion of pseudowords in our stimulus set builds on a previous study, from which we abridged our list of words and graphic images (Bemis and Pylkkänen, 2013). We focused on high-frequency gamma changes (Forseth et al., 2018; Conner et al., 2019; Johnson et al., 2020; Leszczyński et al., 2020) that typically index local cortical processing and are implicated in a range of cognitive processes (Buzsáki and Watson, 2012; Hovsepyan et al., 2020; Packard et al., 2020). An early anterior negative deflection immediately preceding the critical noun in combinatorial contexts (−50 to 100 ms) likely indexes syntactic prediction (Neufeld et al., 2016). Low-frequency power increases have also been noted during the anticipatory window and during phrase composition (Bastiaansen and Hagoort, 2015; Lewis et al., 2016; Segaert et al., 2018) and in a variety of auditory phrase and sentence processing paradigms (Ding et al., 2016; Mai et al., 2016; Keitel et al., 2017, 2018). Therefore, we also evaluated the role of low frequencies during anticipatory composition, focusing on the alpha/beta bands, given the joint involvement of these in the literature and the similar anticipatory dynamics attributed to them. Finally, we asked patients to determine whether the words they heard matched a subsequent image, enabling

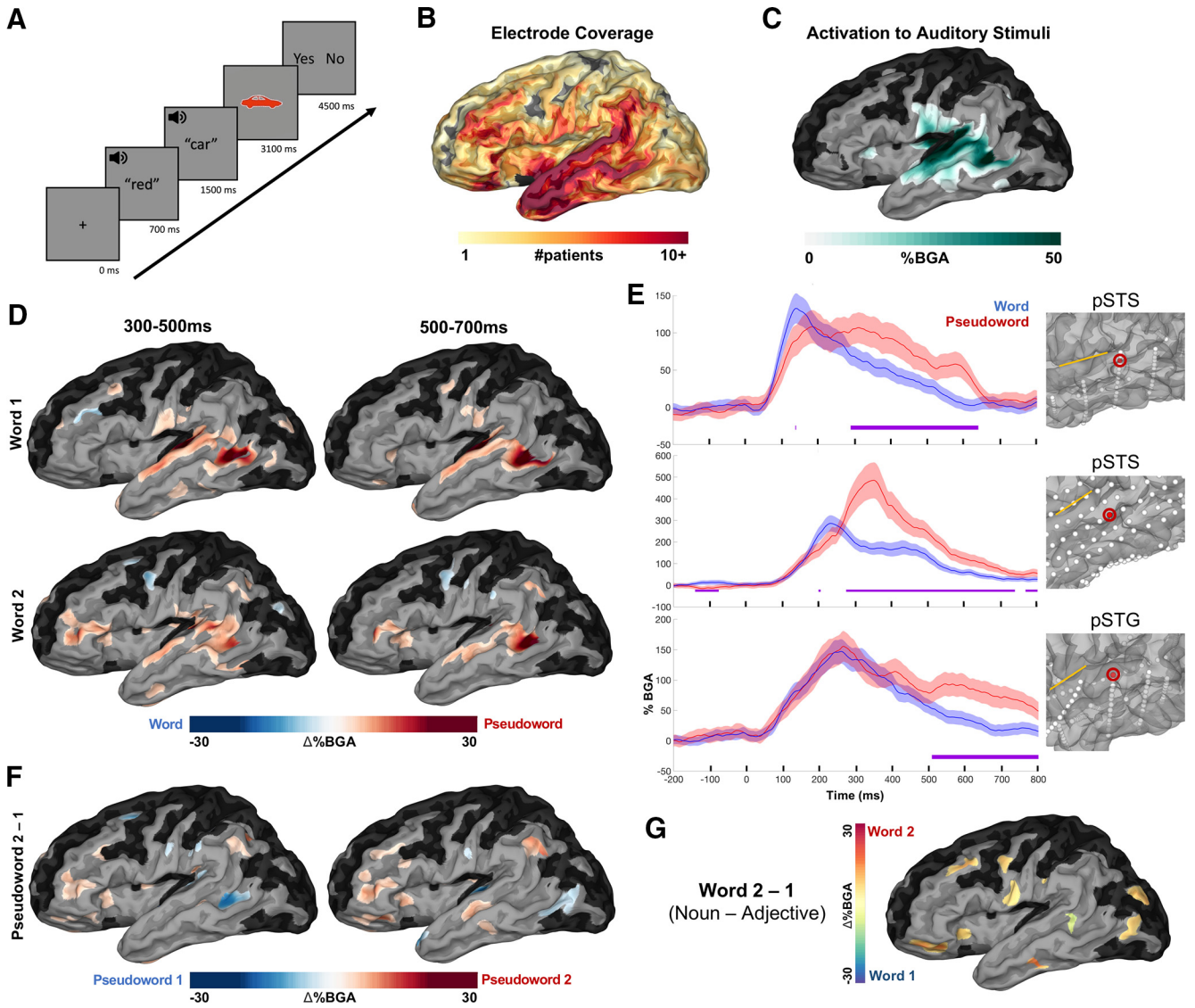

Figure 1. Patient coverage map and grouped analysis for lexicality. ***A***, Experimental design. Average stimuli length: adjectives (420 ± 39 ms; mean ± SD), nouns (450 ± 75 ms), pseudowords (430 ± 38 ms). ***B***, Group coverage map of left hemisph ere electrodes included in analyses, plotted on a semi-inflated standardized N27 surface. ***C***, BGA increases from prestimulus baseline (−500 to −100 ms before first word) for all conditions from 100 to 400 ms after first word onset (threshold: % BGA > 5%, $t > 1.96$, patient coverage ≥ 3; $p < 0.01$ corrected). Black surfaces fell below patient coverage threshold. ***D***, SB-MEMA comparing words versus pseudowords. Red coloration indexes greater BGA (70–150 Hz) for pseudowords and blue for words (same thresholds as in ***C***). Top, Word position 1; bottom, word position 2. ***E***, Exemplar electrodes for the words versus pseudowords analysis. Error bars (colored shading) set at 1 SD. Sylvian fissure is marked with a yellow line for reference on each surface. Time, 0 ms indicates word 1 onset. ***F***, SB-MEMA indicating BGA increases for pseudowords at the second word position relative to pseudowords at the first word position (time windows collapsed for both word 1 and word 2 positions). ***G***, SB-MEMA contrast for real words from both noncompositional conditions across the 300–500 ms window (Adjective-Pseudoword and Pseudoword-Noun).

validation of their attention as well as analyses related to phrase-matched and phrase-contrasted contexts. Our analyses were restricted to language-dominant left-hemisphere electrode coverage.

Participants were presented with two-word auditory phrases, grouped by three conditions, Adjective-Noun (red boat), Adjective-Pseudoword (red neub), and Pseudoword-Noun (zuik boat). Because these pseudoword phrases include phonologically viable nonwords, differences in the second position of the phrase between these items and the grammatical noun phrases are likely a result of compositional processing. Although most previous studies have presented a licensable noun, our inclusion of the Adjective-Pseudoword condition further isolates composition and reduces predictability. To ensure attention was maintained, after each trial participants were shown a colored drawing and asked to press a button indicating whether the picture matched the phrase they had just heard. Participants were told to respond positively only when the picture fully matched the phrase. Auditory and visual stimuli were adapted from a previous red-boat experiment (Bemis and Pylkkänen, 2013), from which we obtained our list of real words and graphic images.

A fixation cross was presented in the center of the screen for 700 ms followed by the first word, and 800 ms later, the second word was presented. At 1600 ms after the onset of the second word, the picture was presented, and 1400 ms after picture presentation, participants were prompted to respond (Fig. 1*A*). Following their response, a blank screen was shown for 1500 ms. Stimuli were presented in a pseudorandom order, with no repetition among items. The number of trials per block across the full experiment was as follows: Adjective-Noun (80), Pseudoword-Noun (40), Adjective-Pseudoword (40). All patients undertook two blocks. Half of the Adjective-Noun trials matched the picture presented (i.e., red boat was heard by the patient, and a picture of a red boat was then presented), and the other half did not match. The following six adjectives were used: black, blue, brown, green, pink, red (length, mean 4.3, SD 0.7; SUBTLEXus log frequency 3.64). The following twenty nouns were used: bag, bell, boat, bone, cane, cross, cup, disk, flag, fork, hand,

heart, house, key, lamp, leaf, lock, plane, shoe, star (length, mean 4.0, SD 0.6; log frequency 3.38; Brysbaert et al., 2012). The following six pseudowords were used: beeg, cresp, kleg, nar, neub, zuik (length, mean 4.0, SD 0.6). Average stimuli length was Adjectives (420 ms), Nouns (450 ms), Pseudowords (430 ms). Stimuli were presented using Psychtoolbox (Kleiner et al., 2007) on a 15.4 inch LCD screen positioned at eye level, two to three feet from the patient. Auditory stimuli were presented using stereo speakers (44.1 kHz, MacBook Pro 2015).

A total of 3458 electrode contacts were implanted in patients; 2135 of these were included for analysis after excluding channels proximal to the seizure onset zone or exhibiting excessive interictal spikes or line noise. Analyses were performed by first bandpass filtering the raw data of each electrode into broadband gamma activity (BGA; 70–150 Hz) following removal of line noise and its harmonics (zero-phase second order Butterworth band-stop filters). Electrodes were also visually inspected for saccade artifacts. A frequency domain bandpass Hilbert transform (paired sigmoid flanks with half-width 1.5 Hz) was applied, and the analytic amplitude was smoothed [Savitzky–Golay finite impulse response (FIR), third order, frame length of 251 ms; MATLAB 2019b, MathWorks]. BGA was defined as percentage change from baseline level; −500 to −100 ms before the presentation of the first word in each trial. Periods of significant activation were tested using a one-tailed t test at each time point and were corrected for multiple comparisons with a Benjamini–Hochberg false detection rate (FDR) threshold of $q < 0.05$, where the q value denotes the standard term given to adjusted p values for FDR significance corrected for multiple comparisons (Benjamini and Hochberg, 1995; Storey, 2011). For the grouped analysis, all electrodes were averaged within each subject, and then the between-subject averages were used.

To provide statistically robust and topologically precise estimates of BGA, and to account for variations in sampling density, population-level representations were created using surface-based mixed-effects multilevel analysis (SB-MEMA; Fischl et al., 1999; Conner et al., 2011; Kadipasaoglu et al., 2014, 2015). This method accounts for sparse sampling, outlier inferences, as well as intra- and inter-subject variability to produce population maps of cortical activity. A geodesic Gaussian smoothing filter (3 mm full-width at half-maximum) was applied. Significance levels were computed at a corrected alpha level of 0.01 using familywise error rate corrections for multiple comparisons. The minimum criterion for the familywise error rate was determined by white-noise clustering analysis (Monte Carlo simulations, 5000 iterations) of data with the same dimension and smoothness as that analyzed (Kadipasaoglu et al., 2014). Results were further restricted to regions with at least three patients contributing to coverage and BGA percentage change exceeding 5%.

Anatomical groups of electrodes were delineated, first, through indexing electrodes to the closest node on the standardized cortical surface (Saad and Reynolds, 2012), and second, through grouping channels into parcellations determined by Human Connectome Project (HCP) space (Glasser et al., 2016). Parametric statistics were used as HCP regions of interest contained more than 30 electrodes. When contrasting experimental conditions, two-sided paired t tests were evaluated at each time point for each region, and significance levels were computed at $q < 0.01$ using an FDR correction for multiple comparisons.

To generate event-related potentials (ERPs), the raw data were bandpass filtered (0.1–50 Hz). Trials were averaged together, and the resultant waveform was smoothed (Savitzky–Golay FIR, third order, frame length of 251 ms). To account for differences in polarity between electrodes, ERPs were converted to root mean square, using a 50 ms sliding window. All electrodes were averaged within each subject and within ROI, and then the between-subject averages were used.

To explore the functional connectivity between ROIs, we used a generalized phase-locking analysis to estimate the dominant spatiotemporal distributions of field activity and the strength of the coupling between them. Phase information was extracted from the downsampled (200 Hz) and wide bandpass filtered data (3–50 Hz; zero-phase eighth order Butterworth bandpass filter) using the generalized phase method (Davis et al., 2020) with a single-sided Fourier transform approach. This method captures the phase of the predominant fluctuations in the wideband signal and minimizes filter-related distortion of the waveform. Phase-locking value (PLV) was calculated as the circular mean (absolute vector length) of the instantaneous phase difference between each electrode pair at each time point and baselined to the prestimulus period −500 to −100 ms before onset of the first word. Statistics were calculated using the mean PLV of correctly answered trials between 0 and 500 ms after second word onset, comparing against a null distribution generated by randomly re-pairing trial recordings across the electrode pairs 500 times. Significant PLV from prestimulus baseline was accepted at a threshold of $p < 0.05$. When computing conditional differences, significance was accepted at $q < 0.05$ using an FDR correction for multiple comparisons.

Data accessibility. The datasets generated from this research are not publicly available because they contain information noncompliant with the Health Insurance Portability and Accountability Act of 1996, and the human participants from whom the data were collected have not consented to their public release. However, they are available on request from the corresponding author. The custom code that supports the findings of this study is available from the corresponding author on request.

Results

Patients were presented with auditory recordings grouped randomly into the following three conditions: Adjective-Noun, Pseudoword-Noun, Adjective-Pseudoword. A subsequent colored image was presented, and patients were tasked to respond, with a button press, if the image matched the phrase or not (Fig. 1*A*). Across the cohort, we had good coverage over lateral and medial temporal lobe, inferior parietal lobe, and inferior frontal regions, with some coverage reaching into other portions of frontoparietal cortex (Fig. 1*B*). We saw activation in response to the auditory stimuli most prominently in superior and middle temporal regions (Fig. 1*C*). Below we report results pertaining to lexicality, phrase anticipation, phrase composition, and linguistic-visual unification.

Behavioral performance

Performance in the image matching task was highly accurate at 97 ± 3% (311 ± 11/320 trials), with an average response time of 1599 ± 539 ms. Only correct trials were analyzed further.

Effects of lexicality

To disentangle single-word semantic effects from those of combinatorial semantics, we probed the difference in representation between words and pseudowords. We generated a surface-based, population-level map of cortical activity using an SB-MEMA (Fischl et al., 1999; Conner et al., 2011; Kadipasaoglu et al., 2014, 2015), a method specifically designed to account for sampling variations in iEEG and minimize effects of outliers. An SB-MEMA contrasting adjectives and pseudowords in word position 1, and nouns and pseudowords in word position 2 (Fig. 1*D*) revealed significantly greater BGA (70–150 Hz) for pseudowords than words in posterior superior temporal gyrus (pSTG; word 1, 300–500 ms: $\beta = 0.88$; $p = 0.006$), posterior superior temporal sulcus (pSTS; word 1, 300–700 ms: $\beta = 0.30$; $p < 0.001$; word 2, 300–700 ms: $\beta = 0.23$; $p < 0.001$) and pars triangularis (word 2, 300–700 ms: $\beta = 0.08$; $p = 0.004$). We found greater BGA increases for pseudowords than words at position 2 than position 1 around pars triangularis and surrounding frontal areas (Fig. 1*F*; pars triangularis, 300–700 ms: $\beta = 0.09$; $p < 0.001$; pSTS, 300–500 ms: $\beta = 0.09$; $p = 0.008$). A Word 2–1 subtraction for both noncompositional trials (Adjective-Pseudoword, Pseudoword-Adjective) revealed no such effects in posterior temporal regions and a BGA increase for nouns over frontal opercular sites (300–500 ms: $\beta = 0.10$; $p = 0.002$; Fig. 1*G*).

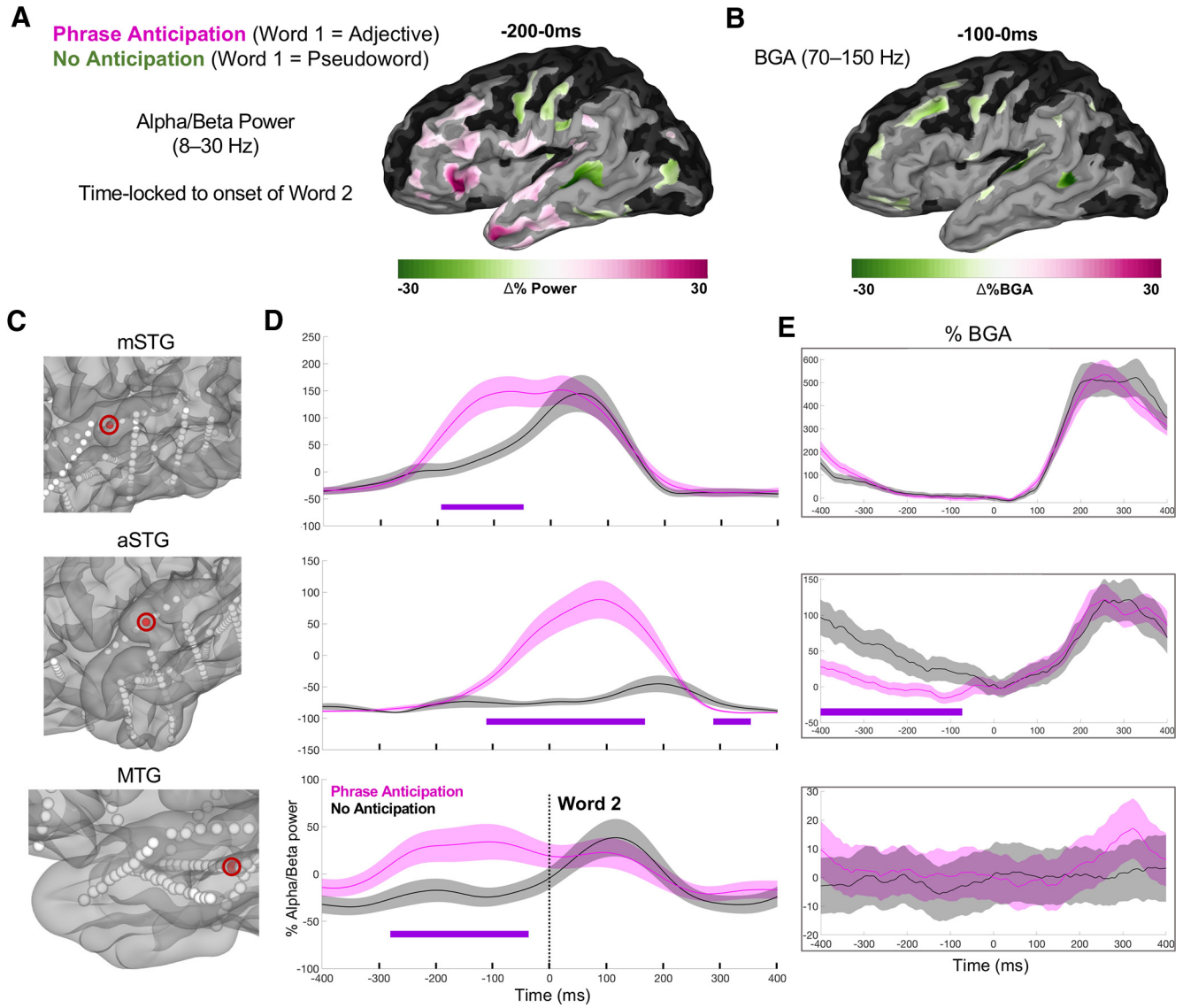

Figure 2. Syntactic-semantic compositional anticipation. ***A***, SB-MEMA for the anticipatory time window centered around second word onset (−200 to 0 ms) for low-frequency alpha/beta power. Pink, Greater power for composition anticipation. Green, Greater for no anticipation (i.e., after having heard a Pseudoword at word 1 position). The same SB-MEMA thresholds as in Figure 1*C* were applied. ***B***, SB-MEMA for BGA for −100 to 0 ms before word 2 onset. ***C***–***E***, Exemplar electrodes with location (***C***), low-frequency power traces (***D***), and BGA traces (***E***) across three patients sorted by row.

Compositional anticipation

We next contrasted Adjective-Noun and Pseudoword-Noun conditions at the onset of second word presentation, with only the former condition licensing any phrasal anticipation. Given that both traditional alpha (8–12 Hz) and beta (12–30 Hz) bands have been regularly implicated in linguistic prediction and anticipatory composition (Lewis et al., 2016; Segaert et al., 2018; Hardy et al., 2021), with previous research in this domain (Gisladottir et al., 2018; Terporten et al., 2019) and neighboring domains (Piai et al., 2020) collapsing these bands into one, we analyzed activity across the 8–30 Hz range. During the anticipatory window for phrase formation (from −200ms to 0 ms before the second word onset), low-frequency power (8–30 Hz) exhibited a significant conditional difference (Fig. 2). Greater alpha/beta power for anticipatory trials was found in pars triangularis (β = 0.18; p = 0.009), ATL (β = 0.15; p = 0.008) and STG (β = 0.13; p = 0.008). These effects were unrelated to BGA. For comparison, we also plot the anticipatory window in BGA for −100 to 0 ms (Fig. 2*B*), which exhibited no clear relation with the lower frequency effects.

Phrase composition

The combinatorial contrast SB-MEMA (Adjective-Noun vs [Adjective-Pseudoword + Pseudoword-Noun]) revealed greater BGA for portions of pSTS during phrase composition than noncomposition (100–300 ms: β = 0.10; p = 0.003; Fig. 3*A*). The specific onset of this effect was ∼210 ms after noun onset, with peak BGA at ∼300 ms (Fig. 4*B*). The same region exhibited greater BGA for noncompositional trials across later windows (300–700 ms: β = 0.10; p = 0.001). Certain portions of pSTS across patients displayed exclusive sensitivity to phrase composition, and not lexicality (Fig. 3*B*,*C*). Other regions—pSTG and IFG—did not show any significant BGA differences between these conditions (Fig. 4*A*). ERP responses were dissociable from BGA across the ROIs plotted; a late effect for noncomposition was

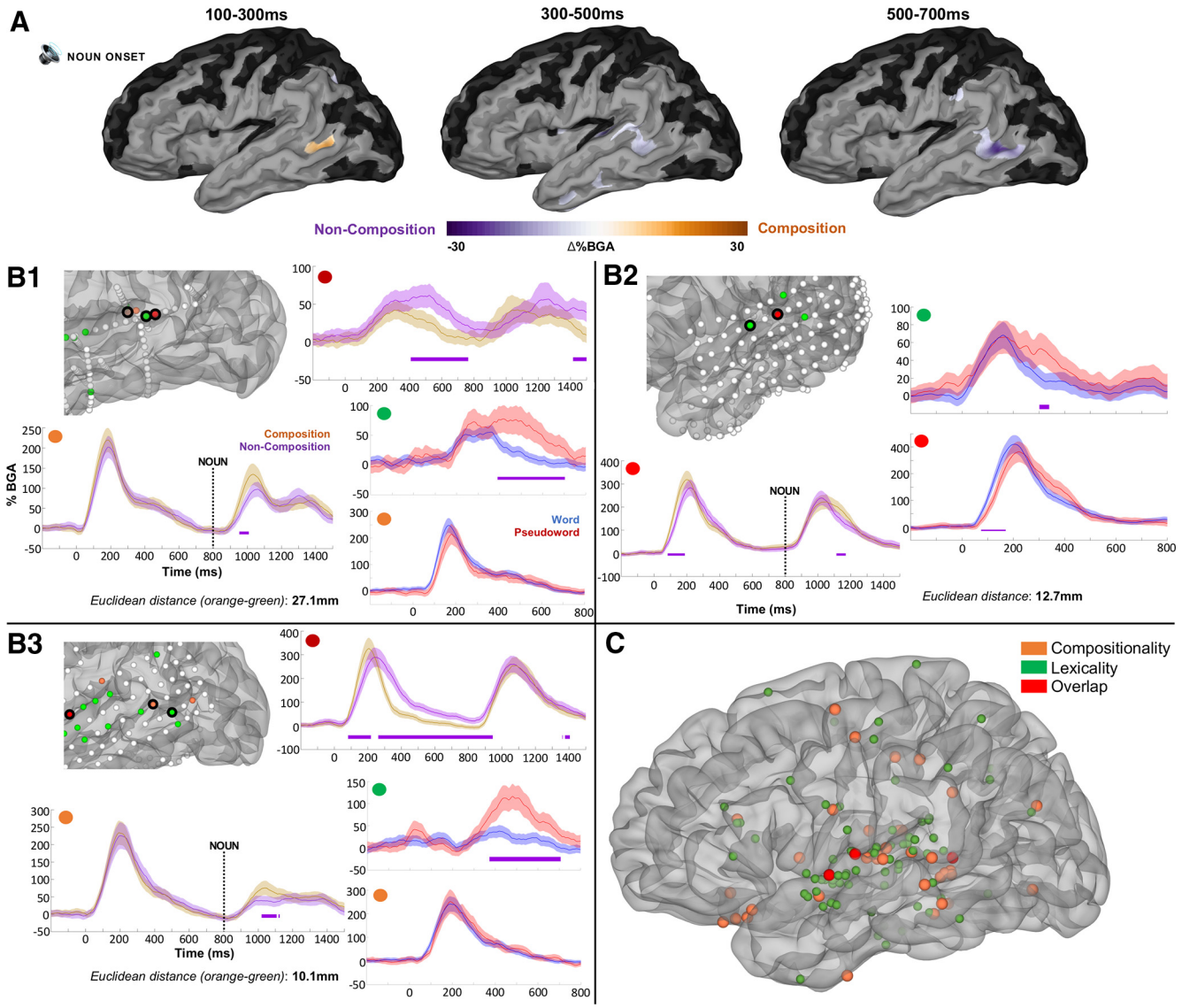

Figure 3. Grouped analysis for phrase composition. ***A***, SB-MEMAs for the phrase composition analysis for BGA (70–150 Hz). Orange indexes greater BGA for phrase composition, and purple indexes greater BGA for noncomposition. The same SB-MEMA thresholds as in Figure 1*C* were applied. Time, 0 ms indicates word 2 onset. ***B***, Exemplar electrodes with FDR-corrected (one-tailed *t* tests, $q < 0.05$) significance bars in purple plotted in native patient space. Includes compositional contrast and lexicality contrast, dissociating neighboring portions of pSTS that responded exclusively for phrase composition and not lexicality (orange dots indicate composition effect; green dots indicate lexicality effect; red dots indicate effect for both composition and lexicality). Electrodes that showed greater, later BGA increases for noncomposition were spatially distinct from those sensitive to composition in early windows. Error bars set at 1 SD. Numbers denote distinct patients (B1–B3). Time, 0 ms indicates word 1 onset; word 2 onset at 800 ms. ***C***, Electrodes exhibiting a significant BGA contrast for compositional versus noncompositional trials, and words versus pseudowords. Thirty-nine electrodes (orange) from 12 patients exhibited an FDR-significant contrast (one-tailed *t* tests, $q < 0.05$) for compositionality at some point between 0 and 1000 ms after the second word; 97 electrodes (green) across 17 patients for lexicality; 3 electrodes (red) for effects of both lexicality and compositionality across 3 patients.

found in Broca's area, and a late signature was detected in temporal pole for composition.

Next, we isolated regions of interest to derive cortical functional connectivity during phrase composition. These were based either on results from our main analysis (pSTS) or on composition effects described in the literature (inferior frontal regions, temporal pole; Graessner et al., 2021b). To characterize functional connectivity between these regions during phrase composition, we computed PLVs for electrode pairs situated within pSTS with either pars triangularis or anterior temporal lobe. We computed the generalized phase of the wideband filtered (3–50 Hz) signal that has previously been shown to be more effective than the use of narrowband alpha or theta filters (Davis et al., 2020).

Among patients with concurrent coverage in pSTS and pars triangularis ($n = 8$, electrode pairs = 231), the majority ($n = 5$) exhibited significantly greater PLVs for compositional than for noncompositional trials during the 0–500 ms period after second word onset, averaging across PLV values for each pair. In patients with joint coverage in pSTS and temporal pole ($n = 8$, electrode pairs = 274), the majority ($n = 6$) showed greater PLVs for the same contrast during the same time window (Fig. 5*A*,*B*). We also contrasted PLVs for compositional electrodes and noncompositional electrodes in pSTS for the subset of patients that had such electrodes. This revealed that compositional electrodes in pSTS exhibited significantly greater PLVs with their paired electrodes in temporal pole and pars triangularis than noncompositional electrodes, with compositional trials also yielding

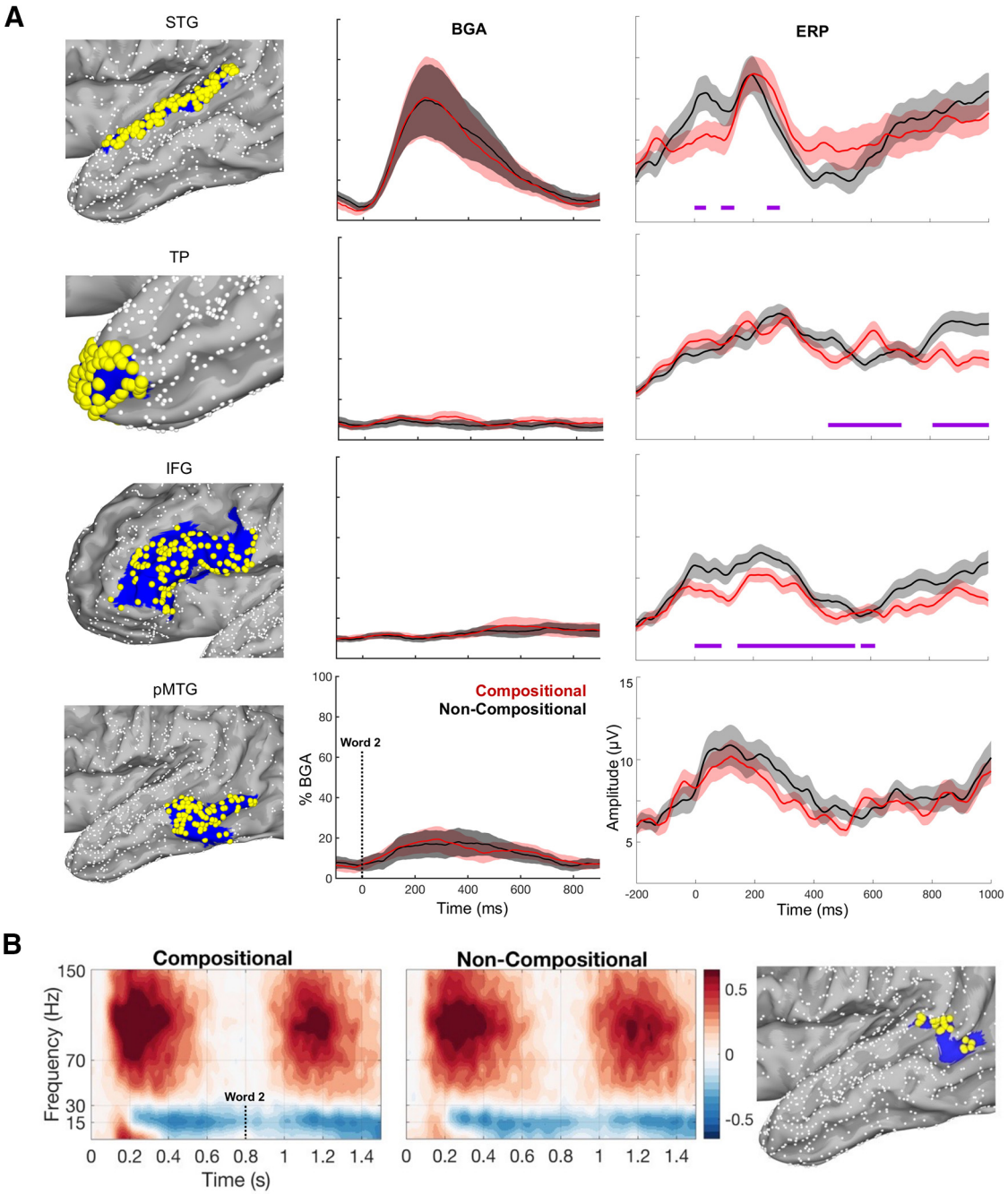

Figure 4. Regions of interest and their broadband high gamma signatures. ***A***, Regions of interest (left) with representations of their broadband gamma activity (middle) and event-related potentials (right). Red, Compositional. Black, Noncompositional. HCP index from top down: pSTG = [A4]; temporal pole = [TGd]; IFG = [FOP4, 44, 45, IFSp, p47r, IFSa, 47l]; pMTG = [PHT, TE1p]. BGA traces are thresholded by $p < 0.05$, significantly active from prestimulus baseline (−500 to −100 ms) with a minimum of 10% BGA amplitude increase during the 100–400 ms window after word 2 onset. ERPs were calculated across the four ROIs plotted on the left column, with significant condition differences being calculated across 0–1000 ms in the same (FDR corrected) manner as the BGA plots. Left, Small white spheres represent electrodes from across all patients that fall outside the region of interest; large yellow spheres represent electrodes included within the region of interest; blue shading represents the HCP surface corresponding to each region of interest. ***B***, Spectrograms and electrodes in pSTS for all active channels (HCP index, TPOJ1; electrodes, 23; patients, 10). pSTS electrode coverage per patient, 1.9 ± 1.4 (mean ± SD). Word 2 onset was at 800 ms.

greater peak PLV values. An exemplar patient for pSTS-pars triangularis connectivity is plotted in Figure 5*C*.

Integration of linguistic and visual information

Comparing the Adjective-Noun trials, which contained a matching versus nonmatching picture, during the 250–500 ms postpicture window SB-MEMAs revealed two notable effects (Fig. 6), that is, the anterior insula ($\beta = 0.16$; $p < 0.001$) and pars triangularis ($\beta = 0.09$; $p = 0.002$) exhibited greater BGA for phrase-picture matches, whereas more dorsal frontal regions, centered around inferior frontal sulcus ($\beta = 0.10$; $p < 0.001$), exhibited greater BGA for phrase-picture nonmatches. Because activity of opercular regions can be misattributed to the insula (Naidich et al., 2004; Woolnough et al., 2019), we ensured that these effects across patients specifically came from electrodes in insula proper by manually checking MRI reconstructions of electrode localizations.

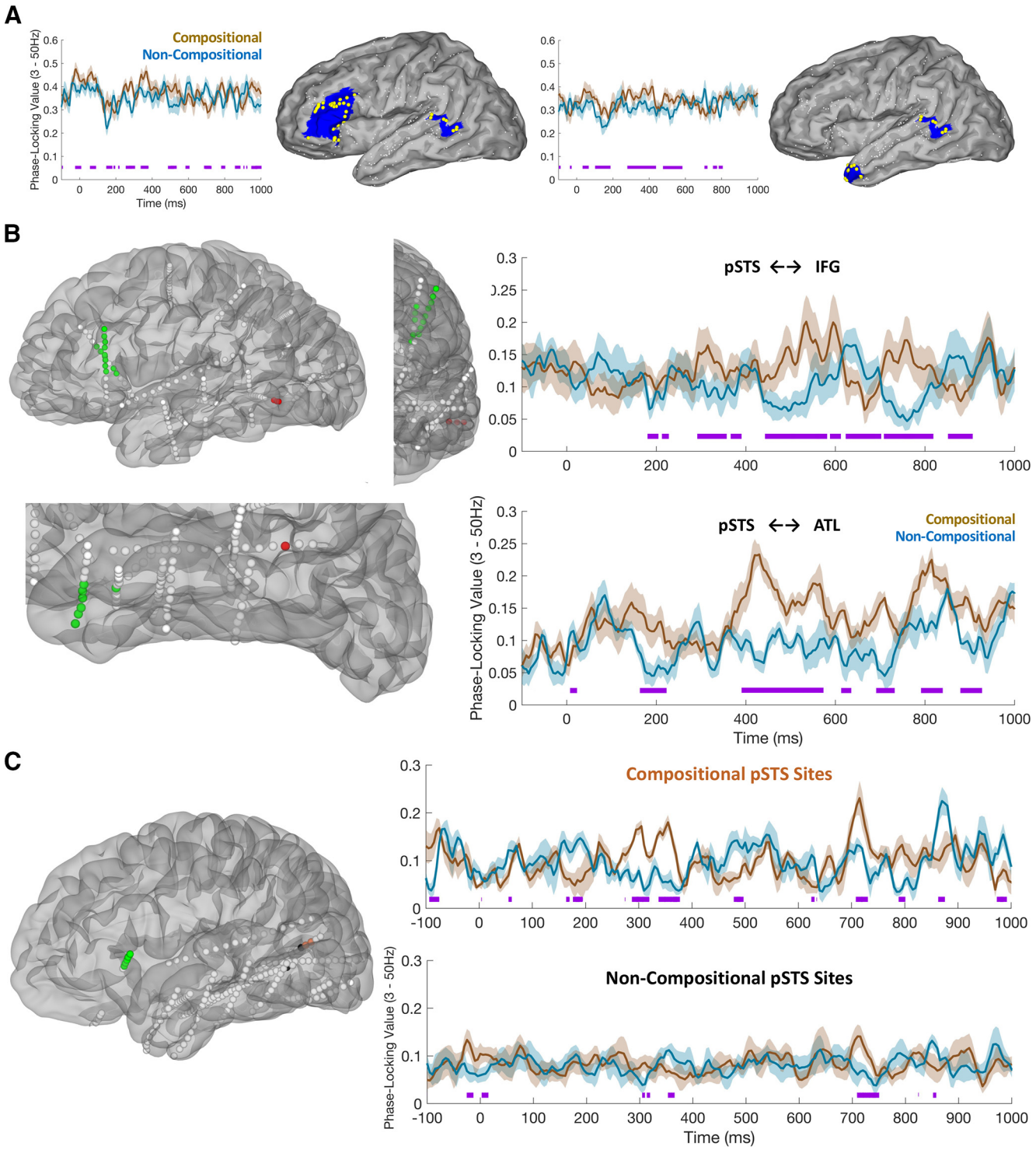

Figure 5. Phase locking between semantic composition regions of interest. ***A***, Left, Average generalized phase-locking values (gPLV) for five patients showing greater gPLV for phrase composition relative to noncomposition between pSTS (HCP index, TPOJ1) and pars triangularis (HCP index, 45, IFSa, IFSp, 47l). Right, Average gPLVs for the six patients showing greater phase locking between pSTS and temporal pole (HCP index, TGd). Purple lines indicate points of significant conditional differences in gPLV values (FDR corrected for multiple comparisons). gPLV values are plotted from prestimulus baseline (−500 to −100 ms before first word onset). In the brain plots, small white spheres represent electrodes from across all patients that fall outside the region of interest; large yellow spheres represent electrodes included within the region of interest; blue shading represents the HCP surface corresponding to each region of interest. ***B***, Posterior temporal lobe (pSTS) gPLVs with inferior frontal gyrus (specifically, pars triangularis, top) and anterior temporal lobe (specifically, temporal pole, bottom). Left, Plots show the localization in native space of electrodes significantly involved ($q < 0.05$) in interregional phase locking (3–50 Hz). Right, Plots show average time courses (mean ± SEM) of phase-locking value changes from baseline in phrase composition (brown) and noncomposition (blue) trials. ***C***, Right, Phase-locking values between pSTS and pars triangularis in an exemplar patient, contrasting PLVs for electrodes in pSTS that showed an effect of phrase composition (top, orange electrodes) with those in pSTS that did not show an effect of composition (bottom, black electrodes). Because pSTS is a small ROI, only a subset of our patients satisfied the criteria for this analysis, that is, those (1) exhibiting joint coverage across pSTS and pars triangularis and (2) having electrodes in pSTS that did show an effect of composition and other electrodes that did not.

Discussion

We localized the neural signatures of phrase comprehension using minimal adjective-noun phrases in a large patient cohort. We identified a broad portion of posterior temporal cortex as being sensitive to lexicality, and identified neighboring portions in pSTS that respond exclusively to phrase composition. This finely organized heterogeneity in responses implies a cortical topography that takes us beyond traditional structure-function mappings for higher order syntax/semantics (Naidich et al., 2004). This mosaic architecture has been ascribed to sensory cortices, and to the best of our knowledge, has not been shown for higher level processing in associative cortices (Fox et al., 2020; Tsao, 2020). We speculate that such organization may be a foundational principle underpinning human language. In this section, we discuss these results in the context of previous findings and evaluate alternative explanations.

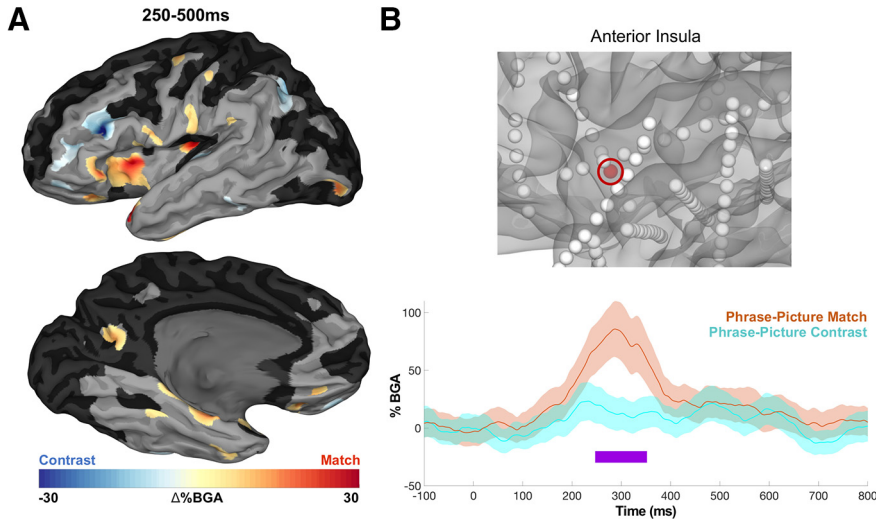

Figure 6. Grouped analysis for linguistic-visual integration. ***A***, SB-MEMA in BGA for phrase-picture match (orange) and phrase-picture contrast (turquoise) increases, 250–500 ms after picture onset (threshold: % BGA $>$ 5%, $t > 1.96$, patient coverage ≥ 3; $p < 0.01$ corrected). ***B***, Exemplar insula electrode.

Anterior portions of IFG exhibited greater BGA for pseudowords at word 2 position relative to word 1, possibly indexing increased unification demands with the preceding adjective (Hagoort, 2005, 2013). This implies a role for IFG in the unification of more or less expected continuations, in agreement with earlier results (Hagoort et al., 2004).

Our results address current concerns in the literature with respect to the spatiotemporal dynamics of phrase composition. Although IFG activity indexes some aspect of phrase anticipation and phrase-picture matching, it is pSTS that appears to encode the earliest responsiveness to meaningful phrases. These results are supported by lesion-behavior mapping research implicating anterior IFG in executive control for decisions on semantic composition and broad portions of MTG in representations of individual phrase constituents (Graessner et al., 2021a).

Last, anterior insula, pars triangularis, and inferior frontal sulcus (IFS) subserve the integration of linguistic input with visual referents. Anterior insula and the IFS have been argued to be the convergence zones of the ventral and dorsal attentional networks (Cazzoli et al., 2021), and our results align with previous models (Willems et al., 2008).

Lexicality

Our results replicate those of prior studies in which BGA localized to m/pSTG, and pSTS tracks lexicality (Tanji et al., 2005; Humphries et al., 2006; Canolty et al., 2007). This activity may index the bundling of lexical features to yield coherent word-level interpretations of auditory stimuli. Our discovery of greater BGA increases for pseudowords than words at position 2 than position 1 around pars triangularis and surrounding frontal areas (Fig. 1*F*) suggests involvement of this region in effortful lexical processing to facilitate semantic unification (Hagoort, 2005, 2013). Greater BGA in posterior temporal regions for pseudowords in position 1 may indicate an effect of auditory repetition suppression, or it may indicate greater processing effort as a function of pseudoword phrase position, that is, greater lexical access effort at position 1 (pSTS) and greater unification effort (IFG) in position 2.

Anticipatory response

Based on our results, we suggest that low-frequency power in IFG and ATL indexes the preparation of a syntactic slot to be filled by predicted upcoming nominal content. Our findings are in line with the notion that beta oscillations can index the construction and maintenance of sentence-level meaning (Lewis et al., 2016) and the claim that alpha/beta increases can index aspects of syntactic anticipation and category generation (Benítez-Burraco and Murphy, 2019; Murphy, 2020).

Minimal phrase composition

We found that neighboring portions of pSTS can exclusively code either for lexicality or phrase composition. Although a large area of posterior and superior temporal cortex was sensitive to lexicality, a narrower portion was recruited exclusively to code for phrase structure (210–300 ms), generating from simple lexical meaning representations of complex meaning (Hagoort, 2020). The same portion of pSTS exhibited greater BGA for noncompositional trials (i.e., pseudowords) at later time points (300–700 ms), implicating it in effortful phrase structure derivations or late-stage lexical search effort/reanalysis. In addition, the greater BGA for phrase composition in pSTS was crucially found across electrodes that were neighboring other pSTS electrodes that showed greater BGA for late-stage pseudoword processing, which we believe contributes to a cortical mosaic. ERP responses were dissociable from BGA. A late effect for noncomposition was found in Broca's area, likely because of greater attempted lexical access for pseudowords, whereas a late signature was detected in temporal pole for composition, potentially related to late-stage conceptual access.

Phrase composition was marked via increased functional connectivity between pSTS electrodes implicated in composition and both inferior frontal regions and temporal pole. This appears to reflect network-level interactions seemingly required for basic phrase formation (Baggio and Hagoort, 2011; Schoffelen et al., 2017). Although the duration of composition effects lasted ~500 ms, there were nevertheless also late-stage periods of brief (~70 ms) reversed effects. Future research involving either denser or fine-grained coverage could provide a clearer picture.

Anatomical connectivity has been elaborated by white matter pathways that connect pSTS with IFG and ATL (Glasser and Rilling, 2008; Figley et al., 2017; Sarubbo et al., 2020). We theorize that the formation of phrase structure in pSTS feeds

categorial information to conceptual interfaces in ATL and memory/control interfaces in pars triangularis. One such piece of information would be the phrase category/label.

Previous intracranial research found that the lower bank of the STS is involved in lexico-semantic processing (Nourski et al., 2021), and our results appear to suggest greater involvement of the lower bank of the pSTS in semantic composition than the cytoarchitechtonically distinct upper bank (Zheng et al., 2010). Future work using higher scale recording techniques, such as single-unit recordings (Bitterman et al., 2008), could address this issue.

One of the main candidates for phrase composition from previous research, ATL, was implicated via late-stage ERPs. ATL activity has been found to be delayed until after intralexical morphologic composition (Flick et al., 2018). This implies the existence of composition-related activity independent of semantic and orthographic processing. Our findings suggest that pSTS might be one such region, although because we only presented auditory stimuli, we cannot make any stronger claims. Our findings are concordant with recent results and models implicating the pSTS in phrase composition (Nelson et al., 2017; Flick and Pylkkänen, 2020; Matchin and Hickok, 2020; Murphy, 2020; Law and Pylkkänen, 2021; Matar et al., 2021), producing hierarchically organized functional morphemes (Lee et al., 2018), sign language comprehension (Trettenbrein et al., 2021), and cross-linguistic reading competence (Feng et al., 2020).

Existing models have posited distinct neural sites across gross portions of the cortical mantle for lexicality and basic composition. Typically, this is a large scale posterior versus anterior temporal (Friederici, 2012) or dorsal versus ventral stream distinction (Bornkessel-Schlesewsky and Schlesewsky, 2013) or a distinction between ATL (conceptual-semantic) and pMTG (hierarchical structure; Matchin and Hickok, 2020). In contrast, we report overlapping functionality at a much smaller scale on the lower bank of the pSTS.

We have claimed that pSTS is tiled in a mosaic-like structure coding for lexicality and phrasal meaning. However, there is an alternative account invoking pseudoword and task-related processing effort. We believe that it is likely that our late-stage (300–700 ms) signature of greater BGA for noncompositional trials in pSTS can be explained by general difficulties with pseudowords. Yet, the effort-related account seems unrelated to our early (100–300 ms) BGA increases for compositional trials; we found no clear posterior temporal differences for real words in noncompositional trials, which the effort-related account would predict (because of nouns being presented after pseudowords). Patients that showed early BGA increases for composition also showed distinct signatures of noncomposition processing effort in neighboring (but distinct) sites in pSTS and surrounding cortex (Fig. 3). A comparison of real-word processing in the noncompositional trials (Fig. 1*G*) revealed no clear effects in posterior temporal regions, only a BGA increase for nouns over frontal opercular sites, suggesting any degree of task-related effort was isolated to late-stage pseudoword processing.

We have provided a more spatiotemporally reliable profile of basic semantic composition than previous noninvasive methodologies, resolving some conflicts in the literature concerning the variety of effect timings documented. In addition, we believe that our results point to the need to move beyond simpler hypotheses about pSTS either being involved in phrase composition or not; instead, it appears to be a question of when and over which specific portions of tissue (e.g., on the order of a few millimeters). We believe that recordings with higher spatial resolution may reveal greater insights into the operations of this cortical mosaic that we have documented.

Although our paradigm allows us to make direct claims about semantic composition, and we suspect that portions of pSTS are also implicated in minimal syntax, however, the functional connectome of the syntax network may differ. Recent work suggests that syntax effects in pSTS are supramodal (Matchin et al., 2022). Given that there is substantial overlap in the distribution of the frontotemporal language network for speakers of 45 languages across 11 language families (Ayyash et al., 2021), and given that the computational process our paradigm isolated was generic, we also suspect that pSTS activity codes for meaningful phrase structures across other languages. The specific neural signatures of basic phrase structure composition isolated here represent an elementary computation in comprehending natural language that can be probed further in future intracranial research.

References

Antonucci S, Beeson P, Labiner D, Rapcsak S (2008) Lexical retrieval and semantic knowledge in patients with left inferior temporal lobe lesions. Aphasiology 22:281–304.

Artoni F, D'Orio P, Catricalà E, Conca F, Bottoni F, Pelliccia V, Sartori I, Russo G, Lo Cappa SF, Micera S, Moro A (2020) High gamma response tracks different syntactic structures in homophonous phrases. Sci Rep 10:7537.

Arya R (2019) Similarity of spatiotemporal dynamics of language-related ECoG high-gamma modulation in Japanese and English speakers. Clin Neurophysiol 130:1403–1404.

Ayyash D, Malik-Moraleda S, Gallée J, Affourtit J, Hoffman M, Mineroff Z, Jouravlev O, Fedorenko E (2021) The universal language network: a cross-linguistic investigation spanning 45 languages and 11 language families. bioRxiv. doi:10.1101/2021.07.28.454040.

Baggio G, Hagoort P (2011) The balance between memory and unification in semantics: a dynamic account of the N400. Lang Cognitive Proc 26:1338–1367.

Bastiaansen M, Hagoort P (2015) Frequency-based segregation of syntactic and semantic unification during online sentence level language comprehension. J Cogn Neurosci 27:2095–2107.

Bemis DK, Pylkkänen L (2011) Simple composition: a magnetoencephalography investigation into the comprehension of minimal linguistic phrases. J Neurosci 31:2801–2814.

Bemis DK, Pylkkänen L (2013) Basic linguistic composition recruits the left anterior temporal lobe and left angular gyrus during both listening and reading. Cereb Cortex 23:1859–1873.

Benítez-Burraco A, Murphy E (2019) Why brain oscillations are improving our understanding of language. Front Behav Neurosci 13:190.

Benjamini Y, Hochberg Y (1995) Controlling the false discovery rate: a practical and powerful approach to multiple testing. J Roy Stat Soc B Met 57:289–300.

Berwick RC, Stabler EP, Berwick RC, Stabler EP (2019) Minimalist parsing. Oxford: Oxford UP.

Bitterman Y, Mukamel R, Malach R, Fried I, Nelken I (2008) Ultra-fine frequency tuning revealed in single neurons of human auditory cortex. Nature 451:197–201.

Bonner MF, Price AR (2013) Where is the anterior temporal lobe and what does it do? J Neurosci 33:4213–4215.

Bornkessel-Schlesewsky I, Schlesewsky M (2013) Reconciling time, space and function: a new dorsal–ventral stream model of sentence comprehension. Brain Lang 125:60–76.

Bozic M, Fonteneau E, Su L, Marslen-Wilson WD (2015) Grammatical analysis as a distributed neurobiological function. Hum Brain Mapp 36:1190–1201.

Brennan J, Pylkkänen L (2012) The time-course and spatial distribution of brain activity associated with sentence processing. Neuroimage 60:1139–1148.

Brennan JR, Stabler EP, Van Wagenen SE, Luh WM, Hale JT (2016) Abstract linguistic structure correlates with temporal activity during naturalistic comprehension. Brain Lang 157–158:81–94.

Brysbaert M, New B, Keuleers E (2012) Adding part-of-speech information to the SUBTLEX-US word frequencies. Behav Res Methods 44:991–997.
Buzsáki G, Watson BO (2012) Brain rhythms and neural syntax: implications for efficient coding of cognitive content and neuropsychiatric disease. Dialogues Clin Neurosci 14:345–367.
Canolty RT, Soltani M, Dalal SS, Edwards E, Dronkers NF, Nagarajan SS, Kirsch HE, Barbaro NM, Knight RT (2007) Spatiotemporal dynamics of word processing in the human brain. Front Neurosci 1:185–196.
Cazzoli D, Kaufmann BC, Paladini RE, Müri RM, Nef T, Nyffeler T (2021) Anterior insula and inferior frontal gyrus: where ventral and dorsal visual attention systems meet. Brain Commun 3:fcaa220.
Chomsky N, Gallego AJ, Ott D (2019) Generative grammar and the faculty of language: insights, questions, and challenges. Catalan J Linguistics: 226–261.
Conner CR, Ellmore TM, Pieters TA, di Sano MA, Tandon N (2011) Variability of the relationship between electrophysiology and BOLD-fMRI across cortical regions in humans. J Neurosci 31:12855–12865.
Conner CR, Kadipasaoglu CM, Shouval HZ, Hickok G, Tandon N (2019) Network dynamics of Broca's area during word selection. PLoS One 14: e0225756.
Cox RW (1996) AFNI: software for analysis and visualization of functional magnetic resonance neuroimages. Comput Biomed Res 29:162–173.
Dale AM, Fischl B, Sereno MI (1999) Cortical surface-based analysis: i. segmentation and surface reconstruction. Neuroimage 9:179–194.
Davis ZW, Muller L, Martinez-Trujillo J, Sejnowski T, Reynolds JH (2020) Spontaneous travelling cortical waves gate perception in behaving primates. Nature 587:432–436.
Ding N, Melloni L, Zhang H, Tian X, Poeppel D (2016) Cortical tracking of hierarchical linguistic structures in connected speech. Nat Neurosci 19:158–164.
Duffau H, Moritz-Gasser S, Mandonnet E (2014) A re-examination of neural basis of language processing: proposal of a dynamic hodotopical model from data provided by brain stimulation mapping during picture naming. Brain Lang 131:1–10.
Feng X, Altarelli I, Monzalvo K, Ding G, Ramus F, Shu H, Dehaene S, Meng X, Dehaene-Lambertz G (2020) A universal reading network and its modulation by writing system and reading ability in French and Chinese children. Elife 9:e54591.
Figley TD, Mortazavi Moghadam B, Bhullar N, Kornelsen J, Courtney SM, Figley CR (2017) Probabilistic white matter atlases of human auditory, basal ganglia, language, precuneus, sensorimotor, visual and visuospatial networks. Front Hum Neurosci 11:1–12.
Fischl B, Sereno MI, Dale AM (1999) Cortical surface-based analysis: II. Inflation, flattening, and a surface-based coordinate system. Neuroimage 9:195–207.
Flick G, Pylkkänen L (2020) Isolating syntax in natural language: MEG evidence for an early contribution of left posterior temporal cortex. Cortex 127:42–57.
Flick G, Oseki Y, Kaczmarek AR, Al Kaabi M, Marantz A, Pylkkänen L (2018) Building words and phrases in the left temporal lobe. Cortex 106:213–236.
Flinker A, Chang EF, Barbaro NM, Berger MS, Knight RT (2011) Sub-centimeter language organization in the human temporal lobe. Brain Lang 117:103–109.
Forseth KJ, Kadipasaoglu CM, Conner CR, Hickok G, Knight RT, Tandon N (2018) A lexical semantic hub for heteromodal naming in middle fusiform gyrus. Brain 141:2112–2126.
Fox NP, Leonard M, Sjerps MJ, Chang EF (2020) Transformation of a temporal speech cue to a spatial neural code in human auditory cortex. Elife 9:e53051.
Friederici AD (2012) The cortical language circuit: from auditory perception to sentence comprehension. Trends Cogn Sci 16:262–268.
Gastaldon S, Arcara G, Navarrete E, Peressotti F (2020) Commonalities in alpha and beta neural desynchronizations during prediction in language comprehension and production. Cortex 133:328–345.
Gisladottir RS, Bögels S, Levinson SC (2018) Oscillatory brain responses reflect anticipation during comprehension of speech acts in spoken dialog. Front Hum Neurosci 12:34.
Glasser MF, Coalson TS, Robinson EC, Hacker CD, Harwell J, Yacoub E, Ugurbil K, Andersson J, Beckmann CF, Jenkinson M, Smith SM, Van Essen DC (2016) A multi-modal parcellation of human cerebral cortex. Nature 536:171–178.
Glasser MF, Rilling JK (2008) DTI Tractography of the human brain's language pathways. Cereb Cortex 18:2471–2482.
Graessner A, Zaccarella E, Friederici AD, Obrig H, Hartwigsen G (2021a) Dissociable contributions of frontal and temporal brain regions to basic semantic composition. Brain Commun 3:fcab090.
Graessner A, Zaccarella E, Hartwigsen G (2021b) Differential contributions of left-hemispheric language regions to basic semantic composition. Brain Struct Funct 226:501–518.
Hagoort P (2003) How the brain solves the binding problem for language: a neurocomputational model of syntactic processing. Neuroimage 20:S18–S29.
Hagoort P (2005) On Broca, brain, and binding: a new framework. Trends Cogn Sci 9:416–423.
Hagoort P (2013) MUC (memory, unification, control) and beyond. Front Psychol 4:416.
Hagoort P (2017) The core and beyond in the language-ready brain. Neurosci Biobehav Rev 81:194–204.
Hagoort P (2020) The meaning-making mechanism(s) behind the eyes and between the ears. Philos Trans R Soc Lond B Biol Sci 375:20190301.
Hagoort P, Hald L, Bastiaansen M, Petersson KM (2004) Integration of word meaning and world knowledge in language comprehension. Science 304:438–441.
Hardy SM, Jensen O, Wheeldon L, Mazaheri A, Segaert K (2021) Modulation in alpha band activity reflects syntax composition: an MEG study of minimal syntactic binding. bioRxiv. doi:10.1101/2021.07.09.451797.
Hovsepyan S, Olasagasti I, Giraud A-L (2020) Combining predictive coding and neural oscillations enables online syllable recognition in natural speech. Nat Commun 11:3117.
Humphries C, Binder JR, Medler DA, Liebenthal E (2006) Syntactic and semantic modulation of neural activity during auditory sentence comprehension. J Cogn Neurosci 18:665–679.
Johnson EL, Kam JWY, Tzovara A, Knight RT (2020) Insights into human cognition from intracranial EEG: a review of audition, memory, internal cognition, and causality. J Neural Eng 17:051001.
Kadipasaoglu CM, Baboyan VG, Conner CR, Chen G, Saad ZS, Tandon N (2014) Surface-based mixed effects multilevel analysis of grouped human electrocorticography. Neuroimage 101:215–224.
Kadipasaoglu CM, Forseth K, Whaley M, Conner CR, Rollo MJ, Baboyan VG, Tandon N (2015) Development of grouped icEEG for the study of cognitive processing. Front Psychol 6:1008.
Keitel A, Ince RAA, Gross J, Kayser C (2017) Auditory cortical delta-entrainment interacts with oscillatory power in multiple fronto-parietal networks. Neuroimage 147:32–42.
Keitel A, Gross J, Kayser C (2018) Perceptually relevant speech tracking in auditory and motor cortex reflects distinct linguistic features. PLoS Biol 16:e2004473.
Kleiner M, Brainard D, Pelli D, Ingling A, Murray R, Broussard C (2007) What's new in psychtoolbox-3. Perception 36:1–16.
Kochari AR, Lewis AG, Schoffelen J-M, Schriefers H (2021) Semantic and syntactic composition of minimal adjective-noun phrases in Dutch: an MEG study. Neuropsychologia 155:107754.
Kohlhase K, Zöllner JP, Tandon N, Strzelczyk A, Rosenow F (2021) Comparison of minimally invasive and traditional surgical approaches for refractory mesial temporal lobe epilepsy: a systematic review and meta-analysis of outcomes. Epilepsia 62:831–845.
Lambon Ralph MA, Ehsan S, Baker GA, Rogers TT (2012) Semantic memory is impaired in patients with unilateral anterior temporal lobe resection for temporal lobe epilepsy. Brain 135:242–258.
Law R, Pylkkänen L (2021) Lists with and without syntax: a new approach to measuring the neural processing of syntax. J Neurosci 41:2186–2196.
Lee DK, Fedorenko E, Simon M, V., Curry WT, Nahed B, V., Cahill DP, Williams ZM (2018) Neural encoding and production of functional morphemes in the posterior temporal lobe. Nat Commun 9:1877.
Leivada E, Murphy E (2021) Mind the (terminological) gap: 10 misused, ambiguous, or polysemous terms in linguistics. Ampersand 8:100073.
Leszczyński M, Barczak A, Kajikawa Y, Ulbert I, Falchier AY, Tal I, Haegens S, Melloni L, Knight RT, Schroeder CE (2020) Dissociation of broadband high-frequency activity and neuronal firing in the neocortex. Sci Adv 6: eabb0977.
Lewis AG, Schoffelen J-M, Schriefers H, Bastiaansen M (2016) A predictive coding perspective on beta oscillations during sentence-level language comprehension. Front Hum Neurosci 10.

Lopopolo A, van den Bosch A, Petersson K-M, Willems RM (2021) Distinguishing syntactic operations in the brain: dependency and phrase-structure parsing. Neurobiol Lang 2:152–175.

Mai G, Minett JW, Wang WS-Y (2016) Delta, theta, beta, and gamma brain oscillations index levels of auditory sentence processing. Neuroimage 133:516–528.

Matar S, Dirani J, Marantz A, Pylkkänen L (2021) Left posterior temporal cortex is sensitive to syntax within conceptually matched Arabic expressions. Sci Rep 11:1–14.

Matchin W, Hickok G (2020) The cortical organization of syntax. Cereb Cortex 30:1481–1498.

Matchin W, İlkbaş aran D, Hatrak M, Roth A, Villwock A, Halgren E, Mayberry RI (2022) The cortical organization of syntactic processing is supramodal: evidence from American Sign Language. J Cogn Neurosci 34:224–235.

McCarty MJ, Woolnough O, Mosher JC, Seymour J, Tandon N (2021) The listening zone of human electrocorticographic field potential recordings. bioRxiv. doi:10.1101/2021.10.22.465519.

Murphy E (2015) Labels, cognomes, and cyclic computation: an ethological perspective. Front Psychol 6:715.

Murphy E (2019) No country for Oldowan men: emerging factors in language evolution. Front Psychol 10:1448.

Murphy E (2020) The oscillatory nature of language. Cambridge: Cambridge UP.

Naidich TP, Kang E, Fatterpekar GM, Delman BN, Gultekin SH, Wolfe D, Ortiz O, Yousry I, Weismann M, Yousry TA (2004) The insula: anatomic study and MR imaging display at 1.5 T. AJNR Am J Neuroradiol 25:222–232.

Nelson MJ, El Karoui I, Giber K, Yang X, Cohen L, Koopman H, Cash SS, Naccache L, Hale JT, Pallier C, Dehaene S (2017) Neurophysiological dynamics of phrase-structure building during sentence processing. Proc Natl Acad Sci U S A 114:E3669–E3678.

Neufeld C, Kramer SE, Lapinskaya N, Heffner CC, Malko A, Lau EF (2016) The electrophysiology of basic phrase building. PLoS One 11:e0158446.

Nourski KV, Steinschneider M, Rhone AE, Kovach CK, Banks MI, Krause BM, Kawasaki H, Howard MA (2021) Electrophysiology of the human superior temporal sulcus during speech processing. Cereb Cortex 31:1131–1148.

Olman CA, Davachi L, Inati S (2009) Distortion and signal loss in medial temporal lobe. PLoS One 4:e8160.

Packard PA, Steiger TK, Fuentemilla L, Bunzeck N (2020) Neural oscillations and event-related potentials reveal how semantic congruence drives long-term memory in both young and older humans. Sci Rep 10:9116.

Piai V, Klaus J, Rossetto E (2020) The lexical nature of alpha-beta oscillations in context-driven word production. J Neurolinguist 55:100905.

Pieters TA, Conner CR, Tandon N (2013) Recursive grid partitioning on a cortical surface model: an optimized technique for the localization of implanted subdural electrodes. J Neurosurg 118:1086–1097.

Pylkkänen L (2020) Neural basis of basic composition: what we have learned from the red-boat studies and their extensions. Philos Trans R Soc Lond B Biol Sci 375:20190299.

Rollo PS, Rollo MJ, Zhu P, Woolnough O, Tandon N (2020) Oblique trajectory angles in robotic stereo-electroencephalography. J Neurosurg 135:245–210.

Saad ZS, Reynolds RC (2012) SUMA. Neuroimage 62:768–773.

Sarubbo S, Tate M, De Benedictis A, Merler S, Moritz-Gasser S, Herbet G, Duffau H (2020) Mapping critical cortical hubs and white matter pathways by direct electrical stimulation: an original functional atlas of the human brain. Neuroimage 205:116237.

Schell M, Zaccarella E, Friederici AD (2017) Differential cortical contribution of syntax and semantics: an fMRI study on two-word phrasal processing. Cortex 96:105–120.

Schoffelen J-M, Hultén A, Lam N, Marquand AF, Uddén J, Hagoort P (2017) Frequency-specific directed interactions in the human brain network for language. Proc Natl Acad Sci U S A 114:8083–8088.

Segaert K, Mazaheri A, Hagoort P (2018) Binding language: structuring sentences through precisely timed oscillatory mechanisms. Eur J Neurosci 48:2651–2662.

Storey JD (2011) False discovery rate. In: International encyclopedia of statistical science. (Lovric M, ed), pp 504–508. Berlin: Springer.

Tanji K, Suzuki K, Delorme A, Shamoto H, Nakasato N (2005) High-frequency gamma-band activity in the basal temporal cortex during picture-naming and lexical-decision tasks. J Neurosci 25:3287–3293.

Terporten R, Schoffelen JM, Dai B, Hagoort P, Kösem A (2019) The relation between alpha/beta oscillations and the encoding of sentence induced contextual information. Sci Rep 9:20255.

Tong BA, Esquenazi Y, Johnson J, Zhu P, Tandon N (2020) The brain is not flat: conformal electrode arrays diminish complications of subdural electrode implantation, a series of 117 cases. World Neurosurg 144:e734–e742.

Trettenbrein PC, Papitto G, Friederici AD, Zaccarella E (2021) Functional neuroanatomy of language without speech: an ALE meta-analysis of sign language. Hum Brain Mapp 42:699–712.

Tsao DY (2020) Does finding a face cell tell us anything much at all? Prog Neurobiol 195:101925.

Uno T, Kawai K, Sakai K, Wakebe T, Ibaraki T, Kunii N, Matsuo T, Saito N (2015) Dissociated roles of the inferior frontal gyrus and superior temporal sulcus in audiovisual processing: top-down and bottom-up mismatch detection. PLoS One 10:e0122580.

Willems RM, Özyürek A, Hagoort P (2008) Seeing and hearing meaning: ERP and fMRI evidence of word versus picture integration into a sentence context. J Cogn Neurosci 20:1235–1249.

Wilson SM, DeMarco AT, Henry ML, Gesierich B, Babiak M, Mandelli ML, Miller BL, Gorno-Tempini ML (2014) What role does the anterior temporal lobe play in sentence-level processing? neural correlates of syntactic processing in semantic variant primary progressive aphasia. J Cogn Neurosci 26:970–985.

Woolnough O, Forseth KJ, Rollo PS, Tandon N (2019) Uncovering the functional anatomy of the human insula during speech. Elife 8:e53086.

Zhang L, Pylkkänen L (2018) Semantic composition of sentences word by word: MEG evidence for shared processing of conceptual and logical elements. Neuropsychologia 119:392–404.

Zheng ZZ, Wild C, Trang HP (2010) Spatial organization of neurons in the superior temporal sulcus. J Neurosci 30:1201–1203.